buildings

MDPI

Article

Bending- and Non-Destructive Tests of Oak (*Quercus* spp.) Glued-Laminated Timber

Mátyás Báder, Róbert Németh *, Dénes Ákos Horváth and Sándor Fehér

Faculty of Wood Engineering and Creative Industries, University of Sopron, Bajcsy-Zsilinszky 4, 9400 Sopron, Hungary; bader.matyas@uni-sopron.hu (M.B.)
* Correspondence: nemeth.robert@uni-sopron.hu

Abstract

This study investigates the mechanical performance and non-destructive evaluation of oak (*Quercus* spp.) glued-laminated timber (GLT), manufactured from predominantly low-quality lamellae (five layers of 20 mm thick lamellae). The other GLT type tested was a veneer-reinforced configuration (4 mm thick veneers in the first and third layers on both sides of the reinforced GLT, combined with five layers of 15 mm thick low-quality lamellae). 18 basic GLT and 5 reinforced GLT beams, with nominal lengths of 2000 mm were produced using polyurethane adhesive and tested under four-point bending, according to EN 408. Their average densities and standard deviations were 759 ± 23 kg/m^3 for basic GLT and 781 ± 6 kg/m^3 for reinforced GLT. The reinforced GLT exhibited a substantially higher modulus of rupture (70.9 ± 4.6 MPa) compared to the basic GLT (37.6 ± 6.2 MPa), representing an increase of 89%. The bending modulus of elasticity also increased by 17.2% (12.0 ± 0.6 vs. 10.3 ± 0.6 GPa). The 11.4–12.0 GPa dynamic modulus of elasticity values were consistent with static results. Strain increased by +66.7% from 0.15% to 0.25% with reinforcement. Despite similar densities, adhesive-related failures governed performance in basic GLT. Veneer reinforcement significantly improved their strength, stiffness, and structural reliability.

Keywords: bending strength; finger joint; GLT; MoR; MoE; NDT; non-destructive testing; oak; veneer reinforcement

1. Introduction

Numerous engineered wood or wood-based products are available now or under development. Cross-laminated timber (CLT), glued-laminated timber (GLT), laminated strand lumber (LSL), laminated veneer lumber (LVL), oriented strand lumber (OSL), solid structural timber (SST or KVH, German: Konstruktionsvollholz) and other product types are promising sustainable construction materials of the future [1,2]. This study focuses on GLT. It can be manufactured with large dimensions and it is increasingly being recognized for its potential in modern architectural design and construction. The shift from small laboratory specimens to large-scale GLT applications presents unique challenges and opportunities in terms of engineering, sustainability, and performance. The utilization of large-dimension GLT in construction projects is driven by its ability to support substantial loads, thereby enabling the design of expansive and open architectural spaces. In addition, it offers a more sustainable, environmentally friendly alternative to concrete-based solutions in many structures. This enhances the versatility of GLT, allowing it to be used in significant

Check for updates

Academic Editors: Jorge Manuel Branco and Minjuan He

Received: 17 April 2026
Revised: 28 July 2026
Accepted: 3 August 2026
Published: 6 August 2026

structural elements such as beams, columns, and trusses in large commercial buildings, bridges, and other civil engineering projects [3–5].

1.1. Using Oak Wood in GLT

Oak wood is particularly advantageous for large-scale GLT applications due to its inherent strength and durability. The high density and mechanical properties of oak, including its modulus of elasticity and bending strength, make it ideal for supporting large loads and spanning wide distances without compromising its structural integrity. Oak retains mechanical stability over time, suggesting a continued suitability for structural applications even as the wood ages [6–8]. Additionally, the esthetic appeal of oak adds value in architecture, where visual impact is as important as structural performance. But oak GLT production presents significant technological and mechanical challenges compared with conventional softwood glulam systems. Its high density, elevated extractive content, limited adhesive penetration, and increased anatomical heterogeneity complicate the bonding process and increase the risk of delamination and brittle failure. The successful bonding of oak requires carefully optimized adhesive systems, particularly polyurethane-based adhesives capable of penetrating dense hardwood tissues [9]. The larger scale of application amplifies challenges such as moisture-related deformations, necessitating careful consideration of environmental conditions [10]. Král et al. [11] reported that hydrothermal exposure significantly affects bond strength in oak laminations, highlighting the sensitivity of hardwood GLT to moisture cycling and adhesive degradation. Moisture-induced damage evolution and delamination in laminated hardwood systems remain major limitations, especially under cyclic climatic loading conditions in laminated beech systems [12]. For oak GLTs bonded with PUR adhesive, performance significantly declines under moisture stress. Pitzner et al. [13] indicate that PUR-bonded oak glulam frequently fails standard delamination requirements at 18% moisture content, with a total delamination as high as 93.4%.

Finger jointing in large-scale applications requires meticulous attention to the integrity of the joint and adhesive performance to ensure that the compounded stresses of large spans do not compromise structural safety [14]. Innovative techniques in joint design and adhesive application are crucial to enhance the mechanical properties of finger-jointed lamellae, supporting their use in large-scale structural elements without sacrificing performance [4]. Finger-jointed oak laminations exhibit lower joint efficiency than softwoods because their anatomical heterogeneity and vessel structure generate stress concentrations. Failure in hardwood GLTs frequently begins at finger joints located in the tension zone, emphasizing the need for optimized joint geometry and lamella grading [15].

However, further research is required with oak, as there is limited published experience with its structural applications and there are no adhesives specifically developed and commercially available. Over the past decades, several studies have examined the use of oak in GLT [16–19], but overall, this number is very small when considered within the broader field of GLT research. Widespread industrial application would require additional studies to address these gaps and explore new possibilities. Certified GLT oak products are already available (Elaborados y Fabricados Gámiz. S.A [20] and Florian Legno s.p.a. [21]). Oak is highly valued for its excellent appearance and physical-mechanical-durability properties. Therefore, it would be advisable to incorporate lower-grade oak timber into GLT production as a strategic choice to optimize cost-effectiveness and resource efficiency [16]. This study aims to address some of these research gaps mainly by bending- and non-destructive tests.

1.2. Improving the Mechanical Performance of GLT Beams

Mechanical performance of GLTs can be improved through strategic placement of lamellae with different strength classes, thicknesses, and stiffness properties within the beam cross-section. Gaff et al. [22] reported that arranging high-quality lamellae in the outer tension and compression zones significantly increases their bending strength and modulus of elasticity, while lower-grade material can be efficiently utilized in the core layers without major reductions in structural performance. Similar findings were presented by Derkowski et al. [23], who demonstrated that the tensile zone may be strengthened by incorporating defect-free timber. Small-sized GLTs reinforced with hardwood face laminations demonstrated approximately 70% greater strength compared with beams manufactured exclusively from pine timber. The targeted positioning of higher-grade laminations and mechanically superior wood species within the tension zone substantially improves the modulus of rupture (*MoR*), while simultaneously decreasing stress concentrations across the beam cross-section. The reinforcement efficiency depends on veneer orientation, thickness, and reinforcement ratio. Finite-element analyses confirm that veneer reinforcement reduces stress concentrations around local material shortages, thereby increasing structural robustness. Experimental investigations also indicate that hybrid GLT–LVL systems exhibit more ductile failure modes than conventional GLT, improving structural reliability under ultimate loading. Combining optimized lamination grading with strategically positioned veneer reinforcement maximizes stiffness, strength, and damage tolerance while maintaining efficient timber utilization [24,25]. *MoR* significantly increased for beams containing plywood in the tension layer, which is the result of the wood species used (birch plywood, pine LVL). The change in structure in the tension zone of beams made of GLT results in an increase in the *MoR* of elements produced in this way [26].

Several investigations also focused on the utilization of low-quality lamellae for sustainable GLT production. Báder et al. [16] examined oak GLTs manufactured entirely from low-quality lamellae containing knots, slope of grain, sapwood, and other defects. Their results showed that mechanical properties can be substantially improved by increasing the number of layers and by introducing defect-free veneer reinforcement in the tensile zone. Multi-layer configurations increased bending resistance by up to 36%, demonstrating that low-grade hardwood resources can be transformed into structurally efficient engineered timber products. Comparable approaches using mixed-grade laminations in softwood and hardwood systems confirmed that overlapping defects and strategic cross-sectional arrangement reduce stress concentrations and homogenize structural behavior [27]. Although the eucalyptus beams exhibited an average density of 813 ± 47 kg/m^3, the hybrid configurations remained significantly lighter, with densities of 516 ± 19 kg/m^3 for eucalyptus-poplar and 545 ± 24 kg/m^3 for enhanced eucalyptus-poplar [28]. Despite their lower density, the enhanced hybrid beams achieved stiffness values approaching those of the fully hardwood eucalyptus configuration, indicating an approximately 33% reduction in density. These findings demonstrate that localized reinforcement and selective upgrading of critical zones can provide high stiffness-to-weight efficiency without requiring full cross-sectional allocation of higher-value materials. However, the increase in stiffness was not accompanied by a corresponding improvement in the *MoR*, suggesting that structural failure remained controlled primarily by critical tensile regions and finger-joint discontinuities rather than by the global elastic stiffness distribution. From another perspective, grade-dependent cross-sectional arrangements are fundamental to GLT, because placing high-strength laminations in the outer tension and compression zones maximizes bending stiffness and strength while reducing material consumption. Heterogeneous layups generally outperform homogeneous layups around openings because stress concentrations are reduced when higher-grade laminations are strategically positioned within the cross-section [29]. Experimental investigations confirm that the spatial distribution of knots and lamina quality significantly influences GLT failure behavior, demonstrating the importance of optimized lamination arrangements rather than average material properties alone [30]. Numerical modeling further indicates that modifying GLT layups can improve bending strength and stiffness without changing the overall beam dimensions, supporting performance-based cross-sectional design [31].

Currently, various non-wood reinforcement technologies are available. Scientific research on reinforced GLT primarily focuses on improving bending strength, stiffness, ductility, and durability through different reinforcement systems [4]. The most common methods involve steel reinforcement, fiber-reinforced polymers, and prestressed composite reinforcements. Steel reinforcement uses embedded rods or plates placed in the tensile zone of glulam beams. This method increases stiffness and ductility while reducing brittle tensile failure. But steel adds weight and may suffer from corrosion and moisture-related compatibility problems with timber [32]. Due to its high tannin content, oak has a strong corrosive effect, so steel bar reinforcement is not recommended. Fiber reinforcement has become increasingly important because of its high tensile strength, corrosion resistance, and low density. Carbon fiber-reinforced polymers provide the greatest mechanical improvement, significantly increasing flexural stiffness of a beam and its load-bearing capacity. Glass fiber-reinforced polymers offer a more economical alternative while still enhancing bending performance and reducing variability of timber [33,34]. Basalt fiber-reinforced polymers are a newer reinforcement solution combining good mechanical performance with improved sustainability and thermal resistance. Experimental studies demonstrate that basalt fiber-reinforced polymers increase stiffness and bending strength while enabling the efficient use of lower-quality timber lamellae [35,36]. Prestressed fiber-reinforced polymer systems further improve GLT performance by reducing tensile stresses, minimizing deflection, and delaying crack formation under loading [37]. The reinforcement methods listed above can be effectively applied to almost any wood species to further improve their performance. The appropriate layer structure and bonding methods still remain critical, similarly to finding adhesives that can form a good bond with both the wood and the reinforcement.

1.3. Mechanical Tests of GLT Beams

The requirements of the EN 14080 [38] standard apply to timber structures, including GLTs. In most cases, this standard relies on the tests specified in EN 408 and the test results obtained. As for most structural elements, the *MoR* from the 4-point bending test and the modulus of elasticity (*MoE*) are critical parameters that dictate the suitability for long spans and heavy loads for large-dimension GLT. Large-scale testing and real-world applications reveal that GLT provides superior performance in bending and shear properties compared to other timber products, largely due to its engineered layered structure and the robustness of its adhesive joints [39]. Accurate modeling and prediction of these properties are essential for designing large structures, ensuring that they can withstand the dynamic loading conditions encountered in real-world environments [40]. GLT beams made from oak wood exhibit a high *MOR*. Studies have shown that oak GLT beams can achieve *MOR* values exceeding 100 N/mm^2, depending on the specific adhesive and reinforcement used [36]. The *MoE* for oak GLT beams typically ranges from 10 to 16 GPa. This high *MoE* suggests that oak GLT beams have a substantial ability to deform elastically under load, which is crucial for large-span applications [36].

The density of oak wood significantly influences the mechanical properties of a GLT. Its higher density correlates with enhanced strength and stiffness, which are critical for supporting large spans and heavy loads. Understanding the distribution of density across different parts of the oak tree, such as the trunk and upper parts of the trunk, is vital for optimizing the mechanical performance of GLT. The density of oak wood used in GLT can vary significantly, with basic density values often ranging from 550 to 700 kg/m^3. Higher densities correlate with increased mechanical strength and stiffness, making oak a suitable material for high-load applications [7,41]. Large-scale applications require careful selection of wood with uniform density to ensure consistent performance across extensive structural elements [42]. Density as well as the dynamic modulus of elasticity (MoE_{dyn}) can be measured using non-destructive testing methods.

1.4. Non-Destructive Testing Methods (NDT)

In large-scale GLT applications, NDT methods are indispensable for monitoring structural conditions. Techniques such as resonance frequency measurement provide detailed insights into the condition of both lamellae and GLT structures, enabling timely identification of wood defects and adhesion problems. There are numerous methods, many of which are also used on an industrial scale. Some of the most important ones are presented below.

The dynamic modulus of elasticity is derived from the fundamental frequencies of vibration of a timber beam. When a beam is excited, it vibrates at its natural frequencies, which are functions of its stiffness and mass distribution. A small impact is typically applied to the timber, and the resulting vibrations are recorded using accelerometers or laser vibrometers. The fundamental frequency is identified, and the dynamic modulus of elasticity is calculated. It provides a quick assessment of the timber's stiffness without causing any damage. It is especially useful for large beams that cannot be easily tested using traditional methods [43,44].

The resonance frequency method involves exciting timber and measuring its resonance frequencies. Each natural frequency corresponds to a specific mode of vibration, which is influenced by the timber's stiffness and geometry. A small impact is applied to the beam, and sensors such as microphones or accelerometers capture the resulting vibration data. The resonance frequencies are identified using Fourier transforms or other signal processing techniques. The MoE_{dyn} is then calculated based on the fundamental frequency and the beam's physical properties. This method is particularly suited for in situ testing of large structural elements [45].

During acoustic emission testing, as timber undergoes stress, micro-cracks or other internal movements generate acoustic waves, which are detected by sensors placed on its surface. The speed and characteristics of these waves are influenced by the material's stiffness and density. Analyzing the waveforms shows the *MoE* [46].

With the stress wave timing method, sensors are attached to the timber, and a known stress is applied. The time taken for the acoustic waves to travel between sensors is measured. This time, combined with the distance between sensors and the density of the timber, allows for calculation of wave velocity. The *MoE* is calculated using the relationship between wave velocity, density and *MoE*. It can detect the initiation of micro-cracks and other defects before they become visible or cause significant damage, allowing for proactive maintenance and repair [47]. These methods are particularly useful for continuous monitoring of large structures, providing real-time data on changes in structural integrity and potential damage development [46].

The specific quantitative accuracy metrics are typically project dependent. The integration of multiple NDT methods enhances accuracy and reliability of the data, offering comprehensive assessments that are crucial for maintaining safety and functionality in large-scale construction projects [48,49]. These methods do not cover all possibilities, but these are important testing techniques. The resonance frequency method was used in this study, which will be described in detail in the Section 2.

https://doi.org/10.3390/buildings16153116

1.5. Lamellae Adhesion for GLT Production

The gluing of oak wood in large-dimension GLT applications demands careful consideration of adhesive characteristics and application techniques. The strength and durability of glue lines are critical in maintaining the structural integrity of large spans, especially under variable environmental conditions [10]. Polyurethane adhesives have proven effective in providing moisture resistance and maintaining bond strength in large-scale applications, supporting the use of oak GLT in demanding construction environments [50]. As an example, shear strength often exceeds 10 N/mm^2 in optimal conditions. Another important issue is that proper surface treatment, such as sanding or planing, enhances the wettability and surface energy of oak wood, leading to improved adhesive performance. The effectiveness of these preparations is often quantified through increased shear strength and reduced failure rates in bonded joints [3,10,51]. The selection and application of adhesives must be optimized to accommodate the increased stress and potential deformations associated with large-scale GLT structures [36].

The shift to large-dimension glued-laminated timber made from oak wood offers potential opportunities for modern construction, providing both structural strength and esthetic appeal. Continued research and innovation in areas such as adhesive technologies, jointing techniques, material selection and non-destructive testing will enhance the performance and sustainability of GLT in large-scale applications. This study explores the properties and applications of GLT, when constructed from low-quality oak wood. It examines critical factors such as 4-point bending strength, modulus of elasticity, density, and non-destructive testing, alongside the specific challenges associated with finger-jointed lamellae in longitudinal applications to fill some research gaps in the field and to open new directions by the utilization of low-quality oak wood.

2. Materials and Methods

2.1. Material Properties and Strength Grading of the Lamellae

The primary raw material was planed hardwood lamella manufactured from high-value oak species (predominantly pedunculate oak and sessile oak, *Quercus* spp.) [52,53], with low quality and with nominal cross-sectional dimensions of 20 × 50 mm and a length of 700 mm parallel to the grain. The material was purchased from Zala-Fűrész Wood Processing and Trading Ltd. (Lenti, Hungary). Owing to limitations in the available stock and to mitigate size effects, it was not feasible to produce a sufficient quantity of 20 mm thick lamellae from the raw material; consequently, 15 mm thick lamellae were additionally produced for a reinforced GLT configuration. The lamellae exhibited various anatomical and growth-related characteristics, including sapwood, the slope of the grain, and in certain instances residual sawn surfaces attributable to reduced thickness (Figure 1). Knots of varying dimensions—both sound and decayed—were also observed. The majority of the pieces corresponded to the appearance grades QF3 and QF4 as defined in EN 975-1 [54], indicating limited suitability for high-grade glued laminated structural members. The second raw material consisted of planed, thin oak boards measuring 4 × 100 × 2000 mm (the final dimension is along the grain), supplied by Lexim Ltd. (Budakeszi, Hungary). Within the scope of this investigation, these thin oak boards are hereafter referred as veneers. The veneers were devoid of visible wood defects, corresponding therefore to the appearance grade QF1 as defined in EN 975-1 [54].

https://doi.org/10.3390/buildings16153116

Figure 1. The lamellae were glued together to form elements. Images (**a**,**b**) show the two sides of some elements. Typical wood defects can be seen such as pin knots, sound knots extending through the full cross-section, decayed knots, slope of grain, cracks, and sapwood.

Following kiln drying, all materials were stored under workshop conditions until reaching an average equilibrium moisture content of 10.7%. Controlled environmental parameters were maintained consistently during manufacturing. Subsequent to planing, the lamellae were longitudinally finger-jointed and edge-glued across their width using a one-component polyurethane adhesive (Henkel LOCTITE HB S209 PURBOND; Henkel AG & Co. KGaA, Düsseldorf, Germany). This process yielded structural elements with cross-sectional dimensions of either 15 or 20 × 100 × 2100 mm, depending on the original thickness of the lamella. Selected adhesive properties were as follows: kinematic viscosity at 20 °C: 17,241–27,586 mm^2/s; dynamic viscosity at 20 °C: 20,000–32,000 mPa·s; density at 20 °C: 1.15–1.17 g/cm^3; maximum permissible wood moisture content: 8%; applicable wood temperature range: 18–35 °C; maximum adhesive layer thickness: 0.1 mm; spread rate: 120–160 g/m^2; open assembly time at 20 °C and 65% RH: 10 min [55,56].

2.2. Geometry and Manufacturing of the GLT Beams

In total, 750 planed lamellae were glued. Across the width of the elements, finger joints were shifted with a 100 mm offset to enhance their structural integrity, because alignment of the joints in a single plane would have produced the lowest load-bearing performance. Each element consisted of six lamellae. All elements were systematically photographed to ensure comprehensive qualitative documentation (Figure 1). Subsequently, the elements were assembled into glued-laminated timber (GLT) beams by face bonding with the same polyurethane adhesive. Due to the length of the lamellae, the finger-jointed connections were not located at mid-span, thereby contributing to its increased load-bearing capacity. All manufacturing procedures were conducted at the production facility of Sokon Ltd. (Agárd, Hungary), a manufacturer of softwood structural GLT beams, employing industrially certified production technology.

The technology and parameters used for oak bonding were consistent with the certified procedures used for the bonding of conifers. Accordingly, proprietary parameters (e.g., pressing conditions) cannot be disclosed in this study. The bonding parameters were in accordance with those specified by the adhesive manufacturer. Two beam configurations were produced. The first sample referred as "basic GLT" (18 beams) constructed exclusively from five layers of 20 mm thick elements, resulting in a cross-section of 99 × 100 mm (width × height). The second sample consisted of five veneer-reinforced beams ("reinforced GLT") with cross-sectional dimensions of 99 × 92 mm (width × height). The difference in the number of specimens may affect the statistical comparison between samples, particularly considering the natural variability the mechanical properties of timber. The reinforced configuration followed a symmetrical layup sequence: 4 mm veneer, 15 mm element, 4 mm veneer, three layers of 15 mm elements, 4 mm veneer, 15 mm element, and 4 mm veneer (Figure 2). Dimensional deviations observed at various production stages can be attributed to pressing tolerances, cumulative adhesive bond-line thickness, and subsequent planing operations. The reduced thickness (15 mm) of a part of the elements incorporated into the reinforced GLT was intentionally selected due to raw material constraints and to mitigate size effects, thereby facilitating a more reliable comparison of the modulus of rupture (*MoR*) and the modulus of elasticity (*MoE*) between the two structural variants. All beams had a nominal length of 2000 mm.

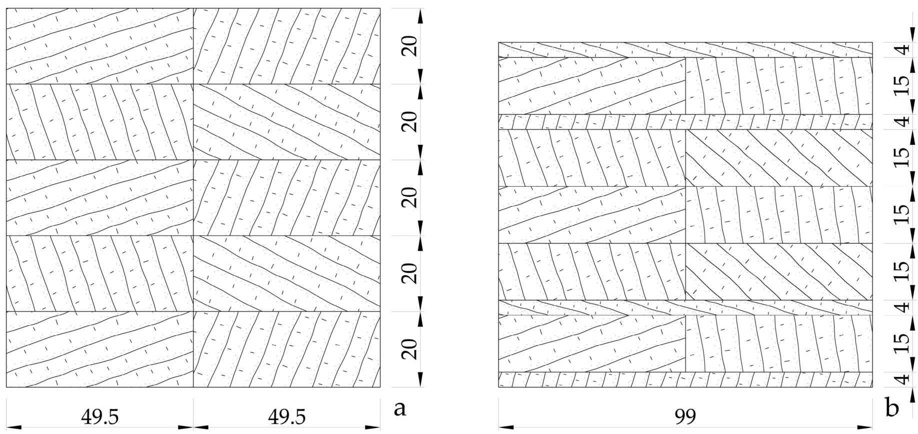

Figure 2. Schematic drawing of the layer structure of (**a**) 5-layer and (**b**) 9-layer samples. All dimensions are given in millimeters.

2.3. Non-Destructive Testing

Following the conditioning to equilibrium moisture content at 20 °C and 65% relative humidity, non-destructive evaluation was performed. The longitudinal natural vibration frequency provides a reliable estimator of the modulus of elasticity [57]. Measurements were conducted using a Portable Lumber Grader Plus instrument (PLG+, Fakopp LLC., Sopron, Hungary), developed for large-scale specimens. The apparatus automatically calculated the density and the dynamic modulus of elasticity (MoE_{dyn}) [58,59]. Vibrations were induced by impact excitation at one end of the specimen using a hammer, while a microphone positioned at the opposite end captured the acoustic signal. The specimens were supported on two vibration-isolating pads to minimize signal interference. Each support incorporated a scale to measure the mass of the specimen, with data transmitted directly to the analysis software. The length of the specimen was recorded automatically using a laser distance sensor, whereas cross-sectional dimensions were measured manually and input into the system. Following signal processing and frequency analysis, the software identified the fundamental longitudinal frequency and computed wave propagation velocity. Their density was derived from mass and geometric dimensions. Subsequently, the MoE_{dyn} was determined from their density and wave velocity. Corrections were applied for influencing parameters, including moisture content [59].

2.4. Static Bending Tests

Thereafter, four-point bending tests were executed in accordance with EN 408:2010 + A1 [60]. The support span (L) was set to 1800 mm, with a load span (L_i) of 600 mm positioned symmetrically, corresponding to the 100 mm specimen depth, using rollers 100 mm in diameter. The veneer-reinforced specimens (92 mm thickness) were tested under identical geometric conditions to ensure comparability. The prescribed ratio $L = 18{\cdot}h \pm 3{\cdot}h$ (where h denotes specimen depth parallel to the bending force) was satisfied: L/h = 18.0 for basic GLT and 19.6 for reinforced GLT, thus complying with the standard requirements. The principal objective was to quantify the difference in load-bearing capacity between the two structural systems. Tests were performed using an Instron 5985 universal testing machine (Illinois Tool Works Inc., Norwood, MA, USA) at a loading rate of 8.0 mm/min, consistent with EN 408:2010 + A1 [60]. Calculations of the *MoR* and the global *MoE* were conducted in accordance with the same standard. The strain (ε) was determined within the linear elastic range, at 40% of the maximum load from the mid-span deflection (w) following da Silva [61] using Equation (1), which assumes a constant bending moment and linear elastic material behavior.

$$\varepsilon = \frac{12{\cdot}h{\cdot}w}{3{\cdot}\mathrm{L}^2 - (\mathrm{L} - \mathrm{L}_i)^2}, \quad (1)$$

Statistical evaluation was carried out by one-way ANOVA at a significance level of 0.05 using Data Science Workbench version 14.2.0.18 (Cloud Software Group Inc., Fort Lauderdale, FL, USA).

3. Results and Discussion

The following parameters were analyzed: density, modulus of rupture (*MoR*), static bending modulus of elasticity (*MoE*), dynamically determined modulus of elasticity (MoE_{dyn}), and strain. On the one hand, the basic GLT and reinforced GLT specimens were evaluated separately to identify intra-group variability and its underlying causes. On the other hand, the basic and reinforced samples were compared directly. Notable that differences in the number of specimens in the two samples can affect the results of the statistical comparisons. Figure 3 presents box plots of the investigated properties.

Except for cracks, the density of components within oak wood exhibits less variation than that observed in coniferous species [62,63]. This primarily applies to knots, contributing to the similarity between 711.2 ± 33.2 kg/m^3 literature values [64–69], defect-free veneer-reinforced specimens (reinforced GLT: 780.9 ± 6.1 kg/m^3), and specimens composed solely of lamellae containing wood defects (basic GLT: 759.2 ± 23.0 kg/m^3). The basic GLT exhibited a higher coefficient of variation (*CV*). It is still limited to 3.03%, primarily attributable to the random occurrence of sapwood, cracks, loose and dead knots, and other material deficiencies. Although the average densities are similar (Figure 3a), their similarity is only weakly significant at a 5% significance level (p = 0.052). When compared with previous research data, the densities of the GLT specimens are in full agreement, including their standard deviations (Table 1).

The reported average *MoR* for small, clear, solid wood specimens is 98.4 ± 17.2 MPa [64–69]. However, due to the substantial size differences and the defect-free, jointless condition of such small specimens, these values are not directly comparable with the results of the present study. In contrast, their *MoE* is a more universal, dimension-independent material property and is less influenced by wood defects [70]; therefore, comparisons with the results of the present study are more meaningful and are discussed below.

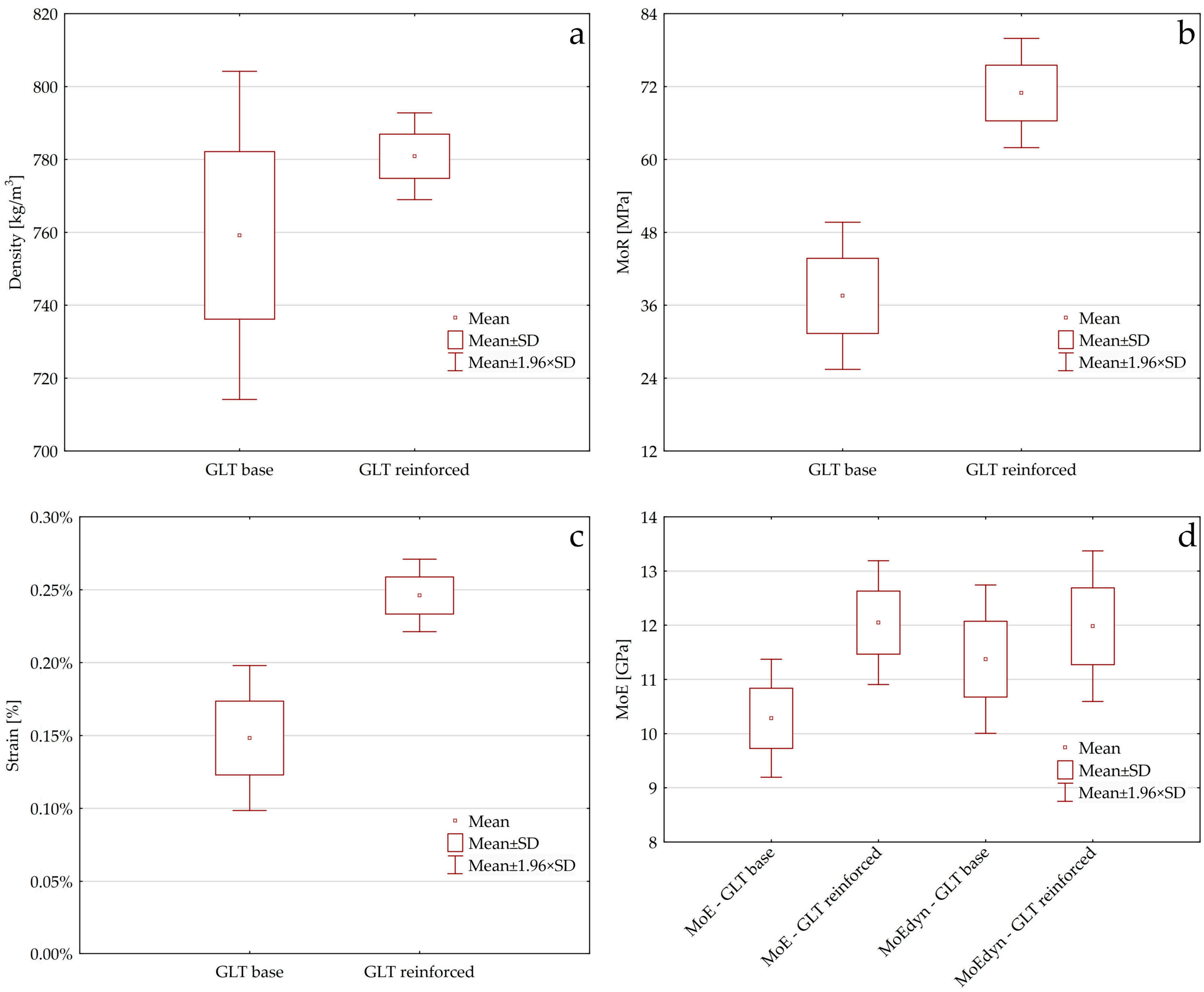

Figure 3. The measured properties of the samples. (**a**) Density; (**b**) modulus of rupture (*MoR*); (**c**) strain; (**d**) static modulus of elasticity (*MoE*) and dynamic modulus of elasticity (MoE_{dyn}) of 5-layer beams (basic GLT) and 9-layer beams (reinforced GLT). SD denotes standard deviation.

Table 1. The 4-point bending test results of oak glued-laminated timbers with different layer structures. The results refer to a moisture content of 12%. Following averages, the standard deviations are shown after the ± sign.

Lamellae Quality	This Study 5-Layers	This Study 9-Layers	Báder et al. [16] 2-Layers	Báder et al. [16] 3-Layers	Báder et al. [16] 4-Layers	Báder et al. [16] 5-Layers	Aicher and Stapf [17] 6-Layers
	Weak Quality Lamellae		Weak Quality Lamellae				Sound Lamellae
Thickness [mm]	100	92	40	45	40	47	120
Density [kg/m^3]	759 ± 23	781 ± 6	764 ± 36	747 ± 22	777 ± 28	767 ± 18	740
MoR [MPa]	37.6 ± 6.2	70.9 ± 4.6	59.0 ± 11.4	63.7 ± 8.9	80.4 ± 5.0	80.0 ± 8.1	54.4 ± 5.7
MoE [GPa]	10.3 ± 0.6	12.0 ± 0.6	11.2 ± 1.4	12.1 ± 1.0	11.3 ± 0.8	11.7 ± 1.0	10.8
MoE_{dyn} [GPa]	11.4 ± 0.7	12.0 ± 0.7	12.6 ± 1.0	12.7 ± 0.9	13.0 ± 1.1	11.9 ± 0.6	n.a.

Abbreviations: *MoR*—modulus of rupture; *MoE*—static modulus of elasticity; MoE_{dyn}—dynamic modulus of elasticity; n.a.—not available. Weak quality lamellae term indicates lamellae corresponding to appearance grades QF3 and QF4 as defined in EN 975-1 [28]. Sound lamellae term indicates appearance grade QF1 (EN 975-1 [28]). The "thickness" refers to the total thickness of the beam.

The average 70.9 MPa *MoR* of the reinforced GLT was 89% higher than that of the basic GLT (Figure 3b). The substantially lower average value of the basic GLT was associated with a higher *CV* of 16.7% compared to the reinforced GLT (6.5%). This clearly reflects the beneficial effect of defect-free veneers in contrast to lamellae containing various wood defects. The more layers provide better overlapping of wood defects [27], and improvement in mechanical performance can also be attributed to the use of defect-free veneers with higher mechanical properties. Notably, only 17.6% was the ratio of the veneer in the reinforced GLT, indicating that a relatively small proportion of high-quality, joint-free wood substantially increase performance, if it is properly positioned within the cross-section. Compared to previous GLT studies, the reinforced GLT exhibited above-average *MoR* values (Table 1), whereas the basic GLT showed the lowest (37.6 MPa). In thinner structures, GLT made from lamellae containing wood defects performed significantly better, reaching bending strengths comparable to those made from sound lamellae (54.4 MPa) [16,17]. In the recent study, failure was predominantly governed by delamination of adhesive layers, typically starting in the outer tensile zone (Figure 4a). Forces acting parallel to bending often led to the opening of finger joints, or occasionally led to failure due to slope of grain, ultimately resulting in the failure of the most highly stressed bonded surfaces. Thus, failure was not primarily caused by wood defects; rather, the performance of the adhesive and the glue lines may have contributed to the premature failure of the beams. In solid wood and layered beams without finger joints, failure typically initiates as brittle fracture on the tension face, propagating through a cascading pattern of longitudinal and transverse tensile failure. The typical failure mode observed for glued beams without finger-joint shows identical crack initiation (by tensile failure of the lower face) but the crack propagation is, sometimes, preferentially appeared through the glued layer interfaces. The finger joint is consistently identified as the critical "weakest link" in structural hardwood assemblies [17,18]. The finger joint is unable to activate the high tensile capacity of superior solid wood, leading to premature fracture at loads below the actual potential of wood. Oak joints often exhibit wood fracture observed at the finger joints, indicating high bond quality, species like beech frequently show adhesive-line separation, which authors attribute to a higher density of 720 kg/m^3 impeding adhesive penetration compared to oak (620 kg/m^3) [17,18]. By the same analogy, these results suggest that the high density of the oak used in this study (759–781 kg/m^3) also inhibits the penetration of the adhesive, leading to the failure of the bonding layers (Figure 4). The ring-porous structure of oak also restricts adhesive penetration [19,71]. But finite element modeling demonstrates that the "lamination effect" of a GLT can postpone total failure even after initial crack onset at a weak finger joint [27]. The datasheet of the adhesive used specifies only softwood species (*Picea abies*, *Abies alba*, *Pinus sylvestris*, *Larix decidua*, *Pseudotsuga menziesii*), explaining its suboptimal performance with oak [55]. In contrast, Horváth and Csiha [51] reported that a one-component structural PUR adhesive can be suitable for hardwood bonding. This suggests that its applicability depends either on the specific adhesive type or the hardwood species, or both. There are also many other influencing factors of the properties of the adhesion. As examples, the adhesive anchorage within the wood substrate; permeability of the wood, because wood with good permeability allows usually better adhesion penetration and thus, better bonding quality; porosity, because it matters how much the adhesive can grip the surface of the material; surface preparation; pressure during the adhesion curing; moisture content of the wood, and other curing conditions. Most of these conditions are specified in the datasheet of the glue, and during the manufacturing these were followed, since the same procedure was used as for conifers. The company manufactures high-quality, certified structural components from conifers, so they are familiar with the use of this type of adhesive. It is also known that adhesives developed for softwoods may not perform adequately even for certain softwood species (e.g., larch, in many cases), let alone with hardwood species. Oak is particularly problematic in this regard. According to Purba et al. [19], both one-component and two-component PUR adhesives represent a formaldehyde-free, eco-friendly alternative for bonding structural oak members. While these systems achieve high shear strength, their effectiveness is often constrained by the high density of oak, the ring-porous structure, the surface acidity, which limit adhesive penetration and the bond integrity [19,71]. The susceptibility of oak to swelling and shrinkage induces high glue-line stresses, so performance significantly declines under elevated moisture content. Research indicates that PUR-bonded oak glulam frequently fails standard delamination requirements at 18% moisture content, with some studies recording total delamination as high as 93.4% [13]. Furthermore, finger joints remain a critical weakness; oak joints bonded with PUR often exhibit failure at the adhesive line rather than wood failure, preventing the full activation of the wood's high tensile potential [13,17]. Consequently, the possibilities available are even more limited for deciduous wood species that are used much less frequently for GLT beams. Optimization may be achieved by specialized manufacturing techniques. The use of primers in combination with PUR adhesive can enhance bond durability [19]. Additionally, hybrid structural members—such as 3-ply CLT with oak outer layers and a poplar middle layer—have demonstrated superior resistance to delamination compared to pure oak specimens, offering a promising approach for structural hardwood applications [19]. An alternative approach is to develop suitable adhesives. Only recently have wood adhesives been developed for a broader range of species, and most commercially available products are still optimized for traditional softwoods [3,72].

a

b

Figure 4. Typical bending test failure of GLTs made exclusively of oak lamellae (**a**) and of oak lamellae reinforced with veneer layers (**b**).

The reinforced GLT incorporated a beam-length, joint-free veneer layer on the tension side, which significantly reduced delamination during bending. This configuration yielded superior performance: the beam-length veneer acted as a unifying element, effectively restraining the opening of finger joints, similarly to a tension tie. A comparable effect was observed in lamellae with grain deviation, where failure occurred only after substantial force (89% higher *MoR*) and deflection due to the restraining effect of the veneer (Figure 4b).

Beyond its superior *MoR* performance, the reinforced GLT demonstrated a lower *CV*. This study clearly demonstrates the potential of using reinforced GLTs. Current design standards as EN 14080 do not yet account for layer configuration, structural composition, or the quality of constituent elements. As hardwood species are increasingly utilized in structural applications, the development and refinement of grading methods will become essential [38,73–77]. Furthermore, the present study highlights that high-performance structural elements can be produced even from lower-quality raw materials. This conclusion is supported by the relatively small differences in the *MoE* values between basic GLT and reinforced GLT samples and the almost identical *CV*, although the *MoE* values are not statistically identical. The fundamental material property—elasticity—indicates similar quality of the material when comparing basic GLT and reinforced GLT.

The average *MoE* of the reinforced GLT was 12.0 ± 0.6 GPa, which is 17.2% higher compared to the basic GLT (Figure 3d). The latter slightly exceeds the literature average for GLTs (11.4 ± 0.4 GPa), indicating that both materials fall within the expected range of elasticity [16,17]. This is further supported by the comparison with solid wood values: the average *MoE* for small, clear oak specimens is 12.6 ± 0.4 GPa [64–69], which is slightly higher than the *MoE* of the reinforced GLT and more notably higher than the basic GLT. This difference is expected, since small, sound specimens generally exhibit superior properties compared to bonded elements made from lower-quality wood.

The lower average of 10.3 GPa *MoE* of the basic GLT and its slightly higher *CV* (5.4%) can be attributed to bonding problems, which may have contributed to lower performance. Micro-cracks at finger joints may have formed even at low deflections within the measurement range of *MoE*, reducing the effective stiffness and resulting in average values only slightly above 10 GPa.

The MoE_{dyn} results provided a more uniform assessment of the specimens (Figure 3d). The transmission of vibrations caused by the hammer impact is impeded along the grain by wood defects; for instance, knots may deflect vibrations, but these vibrations can bypass the knots with relatively low energy loss. As a result, dynamic testing emphasizes the properties of sound wood while partially neglecting defects [78–80]. The average MoE_{dyn} values were 11.4 ± 0.7 GPa for the basic GLT and 12.0 ± 0.7 GPa for the reinforced GLT, closely matching literature values for solid oak GLTs (12.6 ± 0.4 GPa) [16].

The MoE_{dyn}, determined via longitudinal natural vibration frequency measurements, typically yields higher values than static methods [78–80], likely due to its reduced sensitivity to wood defects. From a structural design perspective, this may be considered a limitation. It is essential that in this study, the static and dynamic *MoE* values for the reinforced GLT were identical (12.0 ± 0.6 GPa), with nearly matching standard deviations. This can be attributed to the optimally positioned, high-quality veneer layers. In contrast, the basic GLT exhibited a 10.6% difference between static and dynamic values, consistent with or better than literature findings [78,79,81].

The average strain at 40% of the maximum load for the basic GLT was 0.15% with a *CV* of 17.1%, whereas the reinforced GLT exhibited a significantly higher strain (0.25%) with much lower *CV* (5.2%) (Figure 3c). For defect-free solid oak, the strain at maximum stress ranges between 0.57% and 1.44%, with an average of 1.07% ± 0.27% [66]. As discussed above, the basic GLT failed at 49.0% lower deflections compared to the reinforced GLT due to the failure at finger joints in the tension zone (Figure 4a). The early signs of the failure—for example micro-cracks—likely appeared while the specimen was still within its elastic range. The veneer reinforcement acted as an effective tie on the tension side, holding together lamellae that would otherwise fail prematurely, thereby significantly increasing strain by 66.7%, as well as the maximum load. Although the ability for high deflection is not necessarily advantageous in load-bearing structures, it becomes relevant when associated with substantial increases in load capacity. In such cases, it is essential to verify whether the structure can accommodate the predicted displacements or whether alternative solutions—such as fiber reinforcement in the tension zone—should be employed. Unfortunately, the introduction of additional materials complicates adhesive selection and may reduce environmental sustainability.

Based on density values, the selection of raw materials was appropriate. The underperformance of beams composed of low-quality lamellae—particularly in terms of *MoR*—is primarily attributed to the performance of the adhesive and the glue lines, which may have contributed to the premature failure of the beams, rather than wood defects, based on the observed failure modes. Both static and dynamic *MoE* values remained within the expected ranges, with a low *CV*, although the inferior performance of the basic GLT was still evident.

It would be worthwhile to conduct further tests that would help determine whether the bond strength exceeded the wood strength and whether the mechanical performance of the beams was governed by the veneer reinforcement, the lamellae, or the quality of the bonded interfaces. Thus, both shear strength test in glue line and delamination resistance test should be done.

4. Conclusions

This study assessed the mechanical behavior and non-destructive properties of oak (*Quercus* spp.) glued-laminated timber (GLT) manufactured from predominantly low-quality lamellae, with veneer reinforcement (4 mm thick veneers in the first and third layers on both sides combined with five layers of 15 mm thick lamellae) and without veneer reinforcement (five layers of 20 mm thick lamellae). A total of 23 beams (2000 mm long) were tested using longitudinal vibration and four-point bending according to EN 408, enabling a comparison of density, modulus of rupture (*MoR*), modulus of elasticity (*MoE*), dynamic modulus of elasticity (MoE_{dyn}), and strain at 40% of the maximum load.

The results demonstrated that veneer reinforcement significantly enhances structural performance. The average *MoR* and the standard deviation increased from 37.6 $\pm$ 6.2 MPa (basic GLT) to 70.9 $\pm$ 4.6 MPa (reinforced GLT), corresponding to an 89% improvement, while the *CV* decreased from 16.7% to 6.5%. Despite only 17.6% of the cross-section consisting of defect-free veneer, this configuration effectively mitigated premature failure mechanisms, particularly delamination and finger-joint opening in the tension zone. The average *MoE* increased by 17.2% (from 10.3 $\pm$ 0.6 to 12.0 $\pm$ 0.6 GPa), while the 11.4–12.0 GPa MoE_{dyn} closely matched static measurements, especially in reinforced beams. The density of 759–781 kg/m^3 was consistent with the literature and showed a low 3.03% *CV*, confirming appropriate material selection. The relatively low performance, and the failures of basic GLT were primarily attributed to the performance of the adhesive and the glue lines, that may have contributed to the premature failure of the beams rather than inherent wood defects.

Strain increased markedly from 0.15% to 0.25% (+66.7%) with veneer reinforcement, reflecting improved load redistribution and delayed failure. The findings demonstrate that the performance of GLT beams made exclusively from lower grade lamellae is low, while high-performance structural elements can be produced using lower-grade hardwood raw materials when combined with strategically positioned, defect-free reinforcement layers. This approach enhances both their strength and reliability, although further development of adhesives optimized for hardwood species remains essential for broader structural application, while preserving the largely natural character of the product.

Author Contributions: Conceptualization, R.N., S.F. and D.Á.H.; methodology, M.B., S.F. and D.Á.H.; validation, M.B. and D.Á.H.; formal analysis, M.B.; investigation, D.Á.H. and M.B.; resources, R.N. and M.B.; writing—original draft preparation, M.B.; writing—review and editing, M.B., R.N., S.F. and D.Á.H.; visualization, M.B.; supervision, M.B. All authors have read and agreed to the published version of the manuscript.

Funding: This research received no external funding.

Data Availability Statement: The original contributions presented in this study are included in the article. Further inquiries can be directed to the corresponding author.

Acknowledgments: We are grateful to Zala-Fűrész Wood Processing and Trading Ltd. (Lenti, Hungary) and Lexim Ltd. (Budakeszi, Hungary) for providing the raw materials and to Sokon Ltd. (Agárd, Hungary) for manufacturing the specimens.

Conflicts of Interest: The authors declare no conflicts of interest.

References

1. Song, J.; Chen, C.; Zhu, S.; Zhu, M.; Dai, J.; Ray, U.; Li, Y.; Kuang, Y.; Li, Y.; Quispe, N.; et al. Processing Bulk Natural Wood into a High-Performance Structural Material. *Nature* **2018**, *554*, 224–228. [CrossRef] [PubMed]
2. Van Acker, J. Opportunities and Challenges for Hardwood Based Engineered Wood Products. In *9th Hardwood Conference Proceedings*; Németh, R., Rademacher, P., Hansmann, C., Bak, M., Báder, M., Eds.; 9th Hardwood Proceedings-Part II; University of Sopron Press: Sopron, Hungary, 2021; Volume 9, pp. 5–14.
3. Konnerth, J.; Kluge, M.; Schweizer, G.; Miljković, M.; Gindl-Altmutter, W. Survey of Selected Adhesive Bonding Properties of Nine European Softwood and Hardwood Species. *Eur. J. Wood Wood Prod.* **2016**, *74*, 809–819. [CrossRef]
4. Naud, N.; Sorelli, L.; Salenikovich, A.; Cuerrier-Auclair, S. Fostering GLULAM-UHPFRC Composite Structures for Multi-Storey Buildings. *Eng. Struct.* **2019**, *188*, 406–417. [CrossRef]
5. Shi, Y.-J.; Mi, J.-X.; Huang, J.-L.; He, F.; Chen, L.-H.; Wan, X.-Q. Study on the Origin and Classification of Two Poplar Species on the Qinghai–Tibet Plateau. *Forests* **2023**, *14*, 1003. [CrossRef]
6. Sonderegger, W.; Kránitz, K.; Bues, C.-T.; Niemz, P. Aging Effects on Physical and Mechanical Properties of Spruce, Fir and Oak Wood. *J. Cult. Herit.* **2015**, *16*, 883–889. [CrossRef]
7. Aicher, S.; Ahmad, Z.; Hirsch, M. Bondline Shear Strength and Wood Failure of European and Tropical Hardwood Glulams. *Eur. J. Wood Wood Prod.* **2018**, *76*, 1205–1222. [CrossRef]
8. Carmona Uzcategui, M.G.; Seale, R.D.; Nistal França, F.J. Physical and Mechanical Properties of Clear Wood from Red Oak and White Oak. *BioResources* **2020**, *15*, 4960–4971. [CrossRef]
9. Karastergiou, S.; Mantanis, G.I.; Skoularakos, K. Green Gluing of Oak Wood (*Quercus Conferta* L.) with a One-Component Polyurethane Adhesive. *Wood Mater. Sci. Eng.* **2008**, *3*, 79–82. [CrossRef]
10. Gržan, T.; Novosel, A.; Špada, V.; Mihulja, G.; Živković, V. Achieving Maximum Strength in Oak Wood (*Quercus Robur*, L.) Bonding: Techniques for Surface Preparation and Adhesive Application. *Eur. J. Wood Wood Prod.* **2025**, *83*, 44. [CrossRef]
11. Král, P.; Klímek, P.; Děcký, D. Comparison of the Bond Strength of Oak (*Quercus* L.) and Beech (*Fagus Sylvatica* L.) Wood Glued with Different Adhesives Considering Various Hydrothermal Exposures. *J. For. Sci.* **2015**, *61*, 189–192. [CrossRef]
12. Hassani, M.M.; Wittel, F.K.; Ammann, S.; Niemz, P.; Herrmann, H.J. Moisture-Induced Damage Evolution in Laminated Beech. *Wood Sci. Technol.* **2016**, *50*, 917–940. [CrossRef]
13. Pitzner, B.; Bernasconi, A.; Frühwald, A. *Verklebung Einheimischer Dauerhafter Holzarten Zur Sicherung von Marktbereichen Im Außenbau*; Universität Hamburg, Institut für Holzphysik und Mechanische Technologie des Holzes: Hamburg, Germany, 2021; p. 74.
14. Rodríguez-Grau, G.; Cordonnier, P.-L.; Navarrete, B.; Montero, C.; Alvarado, C.; Pommier, R.; Rosales, V.; Galarce, C. The Adhesion Performance in Green-Glued Finger Joints Using Different Wood Ring Orientations. *Sustainability* **2024**, *16*, 7158. [CrossRef]
15. Morin-Bernard, A.; Blanchet, P.; Dagenais, C.; Achim, A. Glued-Laminated Timber from Northern Hardwoods: Effect of Finger-Joint Profile on Lamellae Tensile Strength. *Constr. Build. Mater.* **2021**, *271*, 121591. [CrossRef]
16. Báder, M.; Horváth, D.Á.; Fehér, S. Properties of 2–5 Layers Small-Sized Glued-Laminated Timber Using Lower Quality Oak (*Quercus* spp.) Lamellae. *Forests* **2025**, *16*, 1767. [CrossRef]
17. Aicher, S.; Stapf, G. Glulam from European White Oak: Finger Joint Influence on Bending Size Effect. In *Materials and Joints in Timber Structures*; Aicher, S., Reinhardt, H.-W., Garrecht, H., Eds.; Springer: Dordrecht, The Netherlands, 2014; pp. 641–656.

18. Tran, V.; Oudjene, M.; Méausoone, P. Experimental investigation on full-scale glued oak solid timber beams for structural bearing capacity. *Constr. Build. Mater.* **2016**, *123*, 365–371. [CrossRef]
19. Purba, C.Y.C.; Pot, G.; Collet, R.; Chaplain, M.; Coureau, J.-L. Assessment of Bonding Durability of CLT and Glulam Made from Oak and Mixed Poplar-Oak According to Bonding Pressure and Glue Type. *Constr. Build. Mater.* **2022**, *335*, 127345. [CrossRef]
20. Elaborados y Fabricados Gámiz, S.A. Declaration of Performance. Nr. DOP-EYFG-RE-003. VIGAM–Glued Laminated Timber Made from Oak Without Preservative Treatment. ETA-13/0642. 2013, p. 4. Available online: https://www.eota.eu/etassessments/16399 (accessed on 31 May 2026).
21. FLORIAN LEGNO s.p.a. FLO.LAM.OAK. ETAssessment 13/0642. 2025, p. 13. Available online: https://www.florianinc.com/wp-content/uploads/2025/06/ETA-25-0265_ElectCopy.pdf (accessed on 31 May 2026).
22. Gaff, M.; Babiak, M.; Vokatý, V.; Gašparík, M.; Ruman, D. Bending Characteristics of Hardwood Lamellae in the Elastic Region. *Compos. Part B Eng.* **2017**, *116*, 61–75. [CrossRef]
23. Derkowski, A.; Kuliński, M.; Trociński, A.; Kawalerczyk, J.; Mirski, R. Mechanical Characterization of Glued Laminated Beams Containing Selected Wood Species in the Tension Zone. *Materials* **2022**, *15*, 6380. [CrossRef] [PubMed]
24. Aicher, S.; Tapia, C. Novel Internally LVL-Reinforced Glued Laminated Timber Beams with Large Holes. *Constr. Build. Mater.* **2018**, *169*, 662–677. [CrossRef]
25. Lechner, M.; Dietsch, P.; Winter, S. Veneer-Reinforced Timber. In Proceedings of the World Conference on Timber Engineering 2021, Santiago, Chile, 9–12 August 2021. [CrossRef]
26. Dziurka, D.; Derkowski, A.; Wieruszewski, M.; Kuliński, M.; Mirski, R. GL Beams Reinforced with Plywood in the Outer Layer. *Materials* **2022**, *15*, 3976. [CrossRef] [PubMed]
27. Linsenmann, P. *European Hardwoods for the Building Sector (EU Hardwoods)*; Holzforschung Austria: Wien, Austria, 2016; p. 57.
28. Cruz Rodríguez, C.; Bravo, R.; Rescalvo, F.J.; Fuentes-García, Y.; Lafuente-Bolívar, F.J. Mechanical Characterization and Numerical Modelling of Enhanced Hybrid Glulam Beams of Eucalyptus and Poplar for Structural Applications. *Mech. Adv. Mater. Struct.* **2026**, *33*, 2636074. [CrossRef]
29. Okamoto, S.; Akiyama, N.; Araki, Y.; Aoki, K.; Inayama, M. Study on the Strength of Glued Laminated Timber Beams with Round Holes: Difference in Structural Performance between Homogeneous-Grade and Heterogeneous-Grade Timber. *J. Wood Sci.* **2021**, *67*, 8. [CrossRef]
30. Kandler, G.; Lukacevic, M.; Füssl, J. Experimental Study on Glued Laminated Timber Beams with Well-Known Knot Morphology. *Eur. J. Wood Wood Prod.* **2018**, *76*, 1435–1452. [CrossRef]
31. Vafadar, F.; Jaaranen, J.; Fink, G. Probabilistic Numerical Modeling of Glued Laminated Timber Beams—Experimental Validation and Insights into the Potential of Layup Modification. *Eng. Struct.* **2025**, *344*, 121310. [CrossRef]
32. Steiger, R.; Serrano, E.; Stepinac, M.; Rajčić, V.; O'Neill, C.; McPolin, D.; Widmann, R. Strengthening of Timber Structures with Glued-in Rods. *Constr. Build. Mater.* **2015**, *97*, 90–105. [CrossRef]
33. Raftery, G.M.; Rodd, P.D. FRP Reinforcement of Low-Grade Glulam Timber Bonded with Wood Adhesive. *Constr. Build. Mater.* **2015**, *91*, 116–125. [CrossRef]
34. Saad, K.; Lengyel, A. Strengthening Timber Structural Members with CFRP and GFRP: A State-of-the-Art Review. *Polymers* **2022**, *14*, 2381. [CrossRef] [PubMed]
35. O'Neill, C.; McPolin, D.; Taylor, S.E.; Harte, A.M.; O'Ceallaigh, C.; Sikora, K.S. Timber Moment Connections Using Glued-in Basalt FRP Rods. *Constr. Build. Mater.* **2017**, *145*, 226–235. [CrossRef]
36. Karaman, A.; Yesil, H. Investigation of Some Physical and Mechanical Properties of Basalt Fiber-Reinforced Polymer (BFRP) Woven Fabrics and Plaster Mesh (PSM) Reinforced Glued Laminated Oak Lumber. *Drv. Ind.* **2024**, *75*, 419–429. [CrossRef]
37. Wdowiak-Postulak, A. Numerical, Theoretical and Experimental Models of the Static Performance of Timber Beams Reinforced with Steel, Basalt and Glass Pre-Stressed Bars. *Compos. Struct.* **2023**, *305*, 116479. [CrossRef]
38. *EN 14080:2013*; Timber Structures-Glued Laminated Timber and Glued Solid Timber-Requirements. European Committee for Standardization (CEN): Brussels, Belgium, 2013; p. 103.
39. Zhao, H.; Ye, Z. Analytic Elasticity Solution of Bi-Modulus Beams under Combined Loads. *Appl. Math. Mech.* **2015**, *36*, 427–438. [CrossRef]
40. Hadoush, A.; Van Den Boogaard, A.H.; Emmens, W.C. A Numerical Investigation of the Continuous Bending under Tension Test. *J. Mater. Process. Technol.* **2011**, *211*, 1948–1956. [CrossRef]
41. Jakubowski, M.; Dobroczyński, M. Allocation of Wood Density in European Oak (*Quercus robur* L.) Trees Grown Under a Canopy of Scots Pine. *Forests* **2021**, *12*, 712. [CrossRef]
42. Fernandes, C.; Gaspar, M.J.; Pires, J.; Silva, M.E.; Carvalho, A.; Brito, J.L.; Lousada, J.L. Within and Between-Tree Variation of Wood Density Components in Pinus Sylvestris at Five Sites in Portugal. *Eur. J. Wood Wood Prod.* **2017**, *75*, 511–526. [CrossRef]
43. Martins, C.; Dias, A.M.P.G.; Cruz, H. Using Non-Destructive Testing to Predict the Mechanical Properties of Glued Laminated Poplar. *Proc. Inst. Civ. Eng.-Struct. Build.* **2019**, *172*, 661–670. [CrossRef]

44. Klapálek, P.; Melzerová, L.; Plachy, T. Dynamic modulus of elasticity of glued laminated timber beams. *Staveb. Obz.* **2014**, *2014*, 120–124.
45. Melzerová, L.; Kuklík, P. Non-Destructive Tests of Modulus of Elasticity for the Glued Laminated Timber Beams. *Procedia Eng.* **2012**, *48*, 409–412. [CrossRef]
46. Jaskowska-Lemańska, J.; Przesmycka, E. Semi-Destructive and Non-Destructive Tests of Timber Structure of Various Moisture Contents. *Materials* **2020**, *14*, 96. [CrossRef] [PubMed]
47. Martins, C.; Dias, A.M.P.G.; Cruz, H. Blue Gum: Assessment of Its Potential for Glued Laminated Timber Beams. *Eur. J. Wood Wood Prod.* **2020**, *78*, 905–913. [CrossRef]
48. Schimleck, L.; Dahlen, J.; Apiolaza, L.A.; Downes, G.; Emms, G.; Evans, R.; Moore, J.; Pâques, L.; Van Den Bulcke, J.; Wang, X. Non-Destructive Evaluation Techniques and What They Tell Us about Wood Property Variation. *Forests* **2019**, *10*, 728. [CrossRef]
49. Abdollahi-Mamoudan, F.; Ibarra-Castanedo, C.; Maldague, X.P.V. Non-Destructive Testing and Evaluation of Hybrid and Advanced Structures: A Comprehensive Review of Methods, Applications, and Emerging Trends. *Sensors* **2025**, *25*, 3635. [CrossRef] [PubMed]
50. Minelga, D.; Ukvalbergienė, K.; Baltrušaitis, A.; Balčiūnas, G. Adhesion Properties between Polyvinyl Acetate Dispersion and Ammonia Modified Oak Wood. *Mater. Sci.* **2013**, *19*, 164–168. [CrossRef]
51. Horvath, N.; Csiha, C. Bondability of Beech Wood with One-Component Polyurethane Structural Adhesive. *Acta Silv. Lignaria Hung.* **2016**, *12*, 135–144. [CrossRef]
52. Móricz, N.; Illés, G.; Mészáros, I.; Garamszegi, B.; Berki, I.; Bakacsi, Z.; Kámpel, J.; Szabó, O.; Rasztovits, E.; Cseke, K.; et al. Different Drought Sensitivity Traits of Young Sessile Oak (*Quercus petraea* (Matt.) Liebl.) and Turkey Oak (*Quercus cerris* L.) Stands along a Precipitation Gradient in Hungary. *For. Ecol. Manag.* **2021**, *492*, 119165. [CrossRef]
53. Dobó, M.; Cseke, K.; Lakatos, F.; Lados, B.B. Összehasonlító Populációgenetikai Vizsgálatok a Pilis Hegység Kocsánytalan És Molyhos Tölgy Állományaiban. *Erd. Közlemények* **2025**, *15*, 135–150. [CrossRef]
54. *EN 975-1:2009*; Sawn Timber. Appearance Grading of Hardwoods. Part 1: Oak and Beech. European Committee for Standardization (CEN): Brussels, Belgium, 2009; p. 35.
55. Henkel Magyarország Kft. *Biztonsági Adatlap az 1907/2006/EK Módosított Rendelet Szerint. LOCTITE HB S209 PURBOND 1100KG*; Henkel Magyarország Kft.: Budapest, Hungary, 2025.
56. Deutschen Instituts für Bautechnik (DIBt). *Allgemeine Bauaufsichtliche Zulassung/Allgemeine Bauartgenehmigung Nr. Z-9.1-802: Herstellung von Keilzinkenverbindungen mit Berührungslosen Klebstoffauftragssystemen unter Verwendung von 1K-PUR-Klebstoffe LOCTITE HB S049 bis HB S209 PURBOND bzw. LOCTITE HB S049 bis HB S209 ECO PURBOND*; Deutschen Instituts für Bautechnik (DIBt): Berlin, Germany, 2025.
57. Divós, F.; Daniel, I.; Hodasz, E.; Jarasi, J. Experimental Investigation of Thirteen Strength Predictor Parameters of Coniferous Wood. In Proceedings of the 1st European Symposium on Nondestructive Testing of Wood, Sopron, Hungary, 21–23 September 1994; pp. 341–349.
58. Sismándy-Kiss, F. Strength of Structural Lumbers in Relation to Physical Properties (Fűrészáru Szilárdsága és Fizikai Tulajdonságainak Kapcsolata). Ph.D. Dissertation, NyME Cziráki József Faanyagtudományok és Technológiák Doktori Iskola, Sopron, Hungary, 2012.
59. Bejó, L.; Sismándy-Kiss, F.; Divós, F. International practice and Hungarian research regarding structural lumber grading (A fűrészáru szilárdsági osztályozásának nemzetközi gyakorlata és hazai kutatási eredményei). *Anyagvizsg. Lapja* **2022**, *2022*, 27–37.
60. *EN 408:2010+A1:2012*; Timber Structures-Structural Timber and Glued Laminated Timber-Determination of Some Physical and Mechanical Properties. European Committee for Standardization (CEN): Brussels, Belgium, 2012; p. 38.
61. da Silva, R. Equations (Step by Step) for Flexural Tests: Three- and Four-Point Bending. *Zenodo* **2022**. [CrossRef]
62. Pietikäinen, M. Detection of Knots in Logs Using X-Ray Imaging. Ph.D. Dissertation, Technical Research Centre of Finland (VTT), Espoo, Finland, 1996.
63. Weidenhiller, A.; Linsenmann, P.; Lux, C.; Brüchert, F. Potential of Microwave Scanning for Determining Density and Tension Strength of Four European Hardwood Species. *Eur. J. Wood Wood Prod.* **2019**, *77*, 235–247. [CrossRef]
64. Horváth, D.; Fehér, S.; Báder, M. The Potential of Producing High Added Value Structural Timber from Lamellae Waste. Test Results and Analysis. *Wood Res.* **2023**, *68*, 44–57. [CrossRef]
65. Róbert, T. *A Tölgyek Nagy Értékű Hasznosítását Befolyásoló Tényezők Vizsgálata és Összehasonlító Elemzése*; Nyugat-Magyarországi Egyetem: Sopron, Hungary, 2013.
66. Gustafsson, S. The Strength Properties of Swedish Oak and Beech. *Drew. Pr. Nauk. Doniesineia Komun.* **2010**, *53*, 67–83.
67. Molnár, S.; Farkas, P. Oak (penduculate and sessile oak). In *Industrial Wood Species of the World*, 2nd ed.; (Földünk ipari fái 2. kiadás); Molnár, S., Farkas, P., Börcsök, Z., Zoltán, G., Eds.; Faipari Tudományos Egyesület: Sopron, Hungary, 2024; pp. 125–130.
68. Molnár, S.; Varga, M.F.; Fehér, S.; Németh, R. Technical properties of wood (A faanyag műszaki tulajdonságai). In *Wood Industrial Handbook I/Faipari Kézikönyv I.*; Molnár, S., Ed.; Faipari Tudományos Alapítvány: Sopron, Hungary, 2000; pp. 59–88.

69. Wagenführ, R. *Holzatlas (Atlas of Wood)*, 6th ed.; neu bearb. und erw. Aufl.; Fachbuchverlag Leipzig im Hanser Verl: Leipzig, Germany, 2007.
70. Komán, S.; Fehér, S.; Ábrahám, J.; Taschner, R. Effect of Knots on the Bending Strength and the Modulus of Elasticity of Wood. *Wood Res.* **2013**, *58*, 617–626.
71. Glavinić, I.; Boko, I.; Torić, N.; Vranković, J. Application of Hardwood for Glued Laminated Timber in Europe. *J. Croat. Assoc. Civ. Eng.* **2020**, *72*, 607–616. [CrossRef]
72. Kolbe, J.; Koesling, S.; Steinberg, T.; Haupt, J.; Schröder, L.; Vallée, T.; Grunwald, C. Modified Glutine Adhesives for Structural Bonding of Glued-in Rods in Timber Engineering. *Int. J. Adhes. Adhes.* **2026**, *144*, 104164. [CrossRef]
73. *EN 14081-1:2016*; Timber Structures. Strength Graded Structural Timber with Rectangular Cross Section. Part 1: General Requirements. European Committee for Standardization (CEN): Brussels, Belgium, 2016; p. 41.
74. *EN 14358:2016*; Timber Structures-Calculation and Verification of Characteristic Values. European Committee for Standardization (CEN): Brussels, Belgium, 2016; p. 15.
75. *EN 338:2016*; Structural Timber. Strength Classes. European Committee for Standardization (CEN): Brussels, Belgium, 2016; p. 11.
76. *EN 384:2016+A1:2019*; Structural Timber. Determination of Characteristics Values of Mechanical Properties and Density. European Committee for Standardization (CEN): Brussels, Belgium, 2019; p. 18.
77. Lovrić Vranković, J.; Uzelac Glavinić, I.; Boko, I.; Torić, N. An Experimental Investigation on the Tensile Properties Parallel to the Grain of European Hornbeam (*Carpinus betulus* L.) Boards. *Eur. J. Wood Wood Prod.* **2025**, *83*, 130. [CrossRef]
78. Arriaga, F.; Íñiguez-González, G.; Esteban, M.; Divos, F. Vibration Method for Grading of Large Cross-Section Coniferous Timber Species. *Holzforschung* **2012**, *66*, 381–387. [CrossRef]
79. Oberhofnerová, E.; Arnetová, K.; Holeček, T.; Borůvka, V.; Bomba, J. Determination of Correlation between Destructive and Nondestructive Test Methods Applied on Modified Wood Exposed to Natural Weathering. *BioResources* **2016**, *11*, 5155–5168. [CrossRef]
80. Nowak, T.; Patalas, F.; Karolak, A. Estimating Mechanical Properties of Wood in Existing Structures—Selected Aspects. *Materials* **2021**, *14*, 1941. [CrossRef] [PubMed]
81. Baar, J.; Tippner, J.; Rademacher, P. Prediction of Mechanical Properties-Modulus of Rupture and Modulus of Elasticity-of Five Tropical Species by Nondestructive Methods. *Maderas Cienc. Tecnol.* **2015**, *17*, 239–252. [CrossRef]

https://doi.org/10.3390/buildings16153116